Nanoparticle Aerogels

International Edition: DOI: 10.1002/anie.201508972
German Edition: DOI: 10.1002/ange.201508972

Versatile Aerogel Fabrication by Freezing and Subsequent Freeze-Drying of Colloidal Nanoparticle Solutions

*Axel Freytag, Sara Sánchez-Paradinas, Suraj Naskar, Natalja Wendt, Massimo Colombo, Giammarino Pugliese, Jan Poppe, Cansunur Demirci, Imme Kretschmer, Detlef W. Bahnemann, Peter Behrens, and Nadja C. Bigall**

Abstract: *A versatile method to fabricate self-supported aerogels of nanoparticle (NP) building blocks is presented. This approach is based on freezing colloidal NPs and subsequent freeze drying. This means that the colloidal NPs are directly transferred into dry aerogel-like monolithic superstructures without previous lyogelation as would be the case for conventional aerogel and cryogel fabrication methods. The assembly process, based on a physical concept, is highly versatile: cryogelation is applicable for noble metal, metal oxide, and semiconductor NPs, and no impact of the surface chemistry or NP shape on the resulting morphology is observed. Under optimized conditions the shape and volume of the liquid equal those of the resulting aerogels. Also, we show that thin and homogeneous films of the material can be obtained. Furthermore, the physical properties of the aerogels are discussed.*

Ever since the first synthesis of aerogel structures from colloidal NP building blocks in 2005,[1] there has been much interest in these self-supporting superstructures. This is mostly because of the large surface-to-volume ratio of these monoliths, being close to that of their building blocks, in combination with them being assembled into a self-supported and macroscopic monolith.[2] For the development of macroscopic materials with nanoscopic properties, the formation of this kind of aerogel superstructure is widely recognized to have been a quantum leap, since the macroscopic monoliths exhibit many of the nanoscopic properties, such as size quantization for many different quantum dot building blocks, or plasmon–exciton interactions in mixed aerogels.[3,4] To date, when fabricating aerogels and aerogel-like structures (that is, nanosponges, metal foams),[5,6] chemical gelation (sol–gel), dealloying, or deposition methods are employed to create self-supported structures, followed by subsequent drying or template removal.[2,5,7–9] One major drawback of the conventional aerogel synthesis is that the synthetic route is a multistep procedure,[2,10,11] because the colloidal NPs first need to be destabilized in a controlled way in order to form hydro- or alcogels,[12] and only once these superstructures have formed they can be transformed to aerogels by supercritical drying.[1,2,12] The nano- and microscopic morphologies of the superstructure are strongly dependent on the destabilization step which means that solvents, surfactants, zeta potential, and especially the type of destabilizing procedure/agent are critical parameters for the nanoscopic morphology of the resulting gels, so that the chemical gelation procedure needs to be adjusted for each system.[13–17] The synthesis of aerogels can be time consuming, complex, and expensive. Furthermore, conventional lyogelation methods are frequently accompanied by syneresis effects, so that it is very difficult to synthesize special external shapes, which in turn would be of interest for possible applications. Herein, we propose an alternative assembly method (see Figure 1) based on a physical process. By freezing aqueous NP colloids in situ and subsequent freeze-drying, monolithic aerogels are obtained that consist of a self-supported network of thin platelets building up the gel network, the platelets being mostly 2D assemblies of the NP building blocks. The advantage of our strategy is the suitability for many different NP systems, since there is no chemical selectivity. Under optimum conditions, the volume and shape of the liquid equal the volume and shape of the resulting aerogel. Additionally we show that thin and homogeneous films of the monolith can be obtained.

[*] A. Freytag, Dr. S. Sánchez-Paradinas, S. Naskar, J. Poppe, C. Demirci, Dr. N. C. Bigall
Institut für Physikalische Chemie und Elektrochemie
Leibniz Universität Hannover
Callinstrasse 3A, 30167 Hannover (Deutschland)
E-mail: nadja.bigall@pci.uni-hannover.de

A. Freytag, Dr. S. Sánchez-Paradinas, S. Naskar, N. Wendt, J. Poppe, C. Demirci, I. Kretschmer, Prof. Dr. D. W. Bahnemann, Prof. Dr. P. Behrens, Dr. N. C. Bigall
Laboratorium für Nano- und Quantenengineering (LNQE)
Leibniz Universität Hannover
Schneiderberg 39, 30167 Hannover (Deutschland)

Dr. M. Colombo
Nanochemistry Department, Istituto Italiano di Tecnologia
Via Morego, 30, 16163 Genova (Italien)

G. Pugliese
Istituto Italiano di Tecnologia
Via Morego, 30, 16163 Genova (Italien)

N. Wendt, Prof. Dr. P. Behrens
Institut für Anorganische Chemie, Leibniz Universität Hannover
Callinstrasse 9, 30167 Hannover (Deutschland)

I. Kretschmer, Prof. Dr. D. W. Bahnemann
Institut für Technische Chemie, Leibniz Universität Hannover
Callinstrasse 3, 30167 Hannover (Deutschland)

Prof. Dr. D. W. Bahnemann
Laboratory for Nanocomposite Materials, Department of Photonics, Faculty of Physics, Saint-Petersburg State University, Ulianovskaia street 3, Peterhof, 198504 Saint Petersburg (Russland)

Supporting information and ORCHID(s) from the author(s) for this article are available on the WWW under http://dx.doi.org/10.1002/anie.201508972.

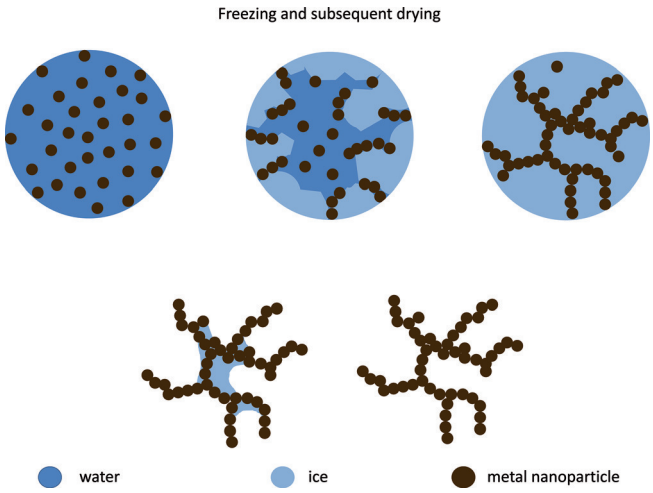

Figure 1. Freezing mechanism (top line) of a droplet of metal nanoparticle colloid in liquid nitrogen from colloidal solution (left) to frozen system (right) and subsequent removal of the ice template (bottom) by lyophilization.

By fast freezing aqueous colloidal NP solutions, which were as droplets injected directly into liquid nitrogen, and by subsequent freeze drying the frozen objects, we obtained highly porous and voluminous monolithic aerogels consisting solely of the respective material. These self-supporting aerogels have densities ranging from 20 to 60 mg cm^{-3}, representing around 0.2 % of the density of the corresponding bulk materials, which is similar to other reported NP aerogels.[18] It should be noted that this equals approximately the volume fraction of the particles in the original colloidal solution. With this method, we were able to synthesize aerogel materials of noble metal NPs, as well as metal oxide and semiconductor NPs. For example, in Figure 2 A, photographs of aerogels are shown, consisting of Au, Ag, Pd, and Pt, as well as of hematite NPs (Fe_2O_3) and of quantum rods (CdS rods grown around CdSe seeds, which are known to exhibit high fluorescence quantum yields and large Stokes shifts).[19,20] This shows a major strength of this method, namely being versatile towards many different NP materials from aqueous solution. Furthermore, this method is also applicable for different ligand molecules. Citrate, thioglycolic acid, and mercaptosuccinic acid covered nanoparticles were for example successfully tested for synthesizing Pt aerogels by means of this cryogelation method (Supporting Information, Section S3). However, it should be noted that when employing fluorescent NPs such as the CdSe/CdS seeded nanorods (Supporting Information, Section S2), the ligand concentration should be low enough to yield a morphology similar to those of other nanoparticles. At the same time the ligand concentration must be high enough to ensure that the resulting monoliths are still fluorescent.

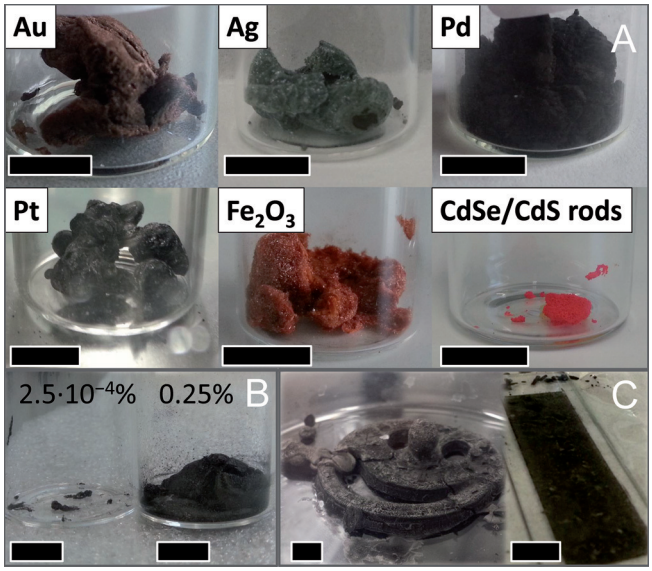

Figure 2. A) Photographs of aerogels of Au, Ag, Pd, Pt, Fe_2O_3, and CdSe/CdS rod-like NPs (scale bar: 1 cm). B) Influence of NP volume fraction of the colloidal solution on the final volume of the monolith, both resulting from 1 mL Pd-colloid (volume fractions of 2.5×10^{-4} % and 0.25 % from left to right, respectively). C) Examples for a variety of shapes possible by cryogelation route: smiley in a Petri dish or thin film on glass slide.

The aerogel monoliths show no shrinkage in comparison to the frozen colloid droplets, if the NP concentration (NP volume fraction) is at least 0.1 % before freezing (Figure 2 B). Instead, a clear shrinkage or collapse of the macroscopic structure was observed, when the volume fraction of the NC concentration was below 0.1 %. Interestingly, for the higher NP concentrations, the shape of the frozen colloid resembles the shape of the resulting aerogel (Figure 2 C). For example, films on glass substrates could be fabricated by the doctor blade method, and other shapes (see "smoking smiley" in Figure 2 C left and Supporting Information) were synthesized. Therefore, our new cryogelation method is advantageous in comparison to conventional aerogels (and xerogels) resulting from lyogelated gels, which are frequently accompanied by syneresis[2,4,7,11,21,22] (i.e. the gels are usually smaller than the colloid liquid). This fact opens the opportunity to create more sophisticated macroscopic shapes. That is, for possible industrial applications the desired shapes can be realized.

In Figure 3, scanning electron (SEM) micrographs and transmission electron (TEM) micrographs of a Pd aerogel are shown in four different magnifications. In general, the microscopic structure of our aerogels consists of highly porous, non-ordered, and well-interconnected networks of 10 nm to 100 nm thin sheets of several μm lengths and widths, (see inset in Figure 3 B) and of wires, which again consist of rolled-up sheets (see Supporting Information, Section S4). Most of the sheets, which build up the free-standing gel network, appear bent, and they exhibit a surface roughness on the nanometer scale. As can be derived from TEM images (Figure 3 C, D), the surface roughness is caused by NPs which are assembled mostly laterally to build up the mesoporous sheets.

In the microscopic regime, the morphologies of the aerogels of different nanomaterials investigated were similar, always consisting of networks of sheet-like assemblies of the NPs and enrolled sheets. The microscopic morphologies were found to be similar for different sizes of the employed nanoparticles (investigated from 3.5 nm to 120 nm diameters)

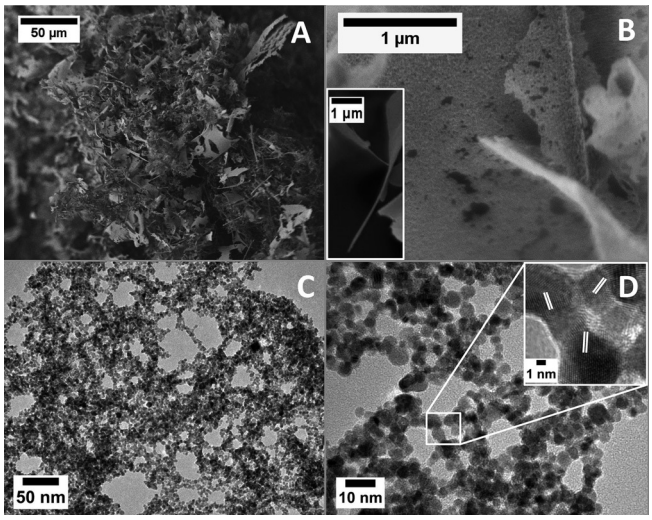

Figure 3. Electron microscope images of a Pd aerogel. SEM images show the interconnected network (A) with a closer look onto the thin sheets (B) and their thickness (inset in B). TEM images reveal mesopores within sheets (C) build of randomly oriented quasi-spherical NPs (D). The inset shows direct contact of the NPs and white bars the (111) face of Pd (lattice distance was measured to be 2.2 Å; previously reported value: 2.246 Å).[23]

and shapes (spheres and rods; Supporting Information, Sections S4–S6) of NPs, materials (Au, Ag, Pt, Pd, hematite, CdSe/CdS), and also for different surface ligands (for example, citrate, mercaptopropionic acid, thioglycolic acid, and chloride ions/hydroxides) as long as the ligand concentrations are low (1 to 2 weight percent; Supporting Information, Section S7) in comparison to the inorganic NP concentration.

For samples such as Pd, Pt, and hematite NPs, as well as CdSe/CdS nanorods, the shapes and sizes of the building blocks are retained, and they assemble randomly oriented to get in contact with each other hence forming the sheet-like structures with free interstitial spaces resulting in high porosity (see Figure 3C, D). We observed an increasing thickness of the nanosheets with higher concentrations (volume fraction) of the colloids employed.

It should be noted that in most but not in all cases the sizes and shapes of the NP building blocks were retained: exceptions were Au and Ag, for which deviations in the crystallite sizes were observed (Supporting Information, Section S4).

Based on our observations from electron microscopy and macroscopic appearances, we postulate the following gelation mechanism for our cryogelation method (see Figure 1): during the fast freezing, the NPs are excluded from the ice crystallites and assemble in the space between them. This effect is supported by the observations and derived model of Zhang et al.,[24] who observed that when freezing NP solutions with high-enough freezing speed, the NPs are not built into the ice crystallites (which in turn only takes place for low freezing speed). This effect has also already been exploited in techniques such as directional freezing.[24,25] In our system, by fast freezing (according to Moor),[26] many small ice crystallites are rapidly formed. Therefore, the NPs are pushed to the crystallite boundaries. A continuous network of the crystallite boundaries filled with NPs is built, which is responsible for the self-supporting nature of the aerogel after ice template removal. A critical NP concentration is needed to form a sheet network with sufficient mechanical stability for providing a self-supported monolith. The observed strong shrinkage at lower NP concentrations is attributed to a poor interconnection of NPs and NP sheets with each other. The higher the NP concentration before freezing, the more NPs are driven in the space between the ice crystals, resulting in thicker assemblies and hence thicker sheets in the aerogel network (see also the Supporting Information, Section S6). The ice removal in the cryogelation process has to be performed by freeze drying to circumvent capillary forces, which appear at the liquid phase and which would lead to destruction of the filigree network.

To date, the highest specific surface area measured by nitrogen adsorption measurements and also by electrochemical methods is in the order of 33 $m^2 g^{-1}$ (6.4×10^3 $m^2 mol^{-1}$), which was measured for a Pt NP aerogel from a 0.025 vol% concentrated solution. This is in the same order of magnitude as the maximum specific surface geometrically estimated for the same NP size (3.5 nm quasi-spherical particles) of 74 $m^2 g^{-1}$. The specific surface area of these aerogels is hence comparable to other metal foams (9 to 81 $m^2 g^{-1}$)[6,27] and (bi)metallic aerogels (46 to 92 $m^2 g^{-1}$).[28–30] The nitrogen adsorption measurements also confirmed the presence of macro- and mesopores (for detailed discussion of nitrogen adsorption and electrochemical measurements, see the Supporting Information, Section S8). From the external dimensions of our aerogels and their total mass, the porosity was estimated to be 99.4% for Pd and 99.7% for Pt, Ag and Au aerogels.

In Figure 4, some of the specific properties obtained of the different NP aerogels are highlighted (for a detailed discussion of the various aerogels, see the Supporting Information, Section S9). The aerogels as synthesized from CdSe/CdS

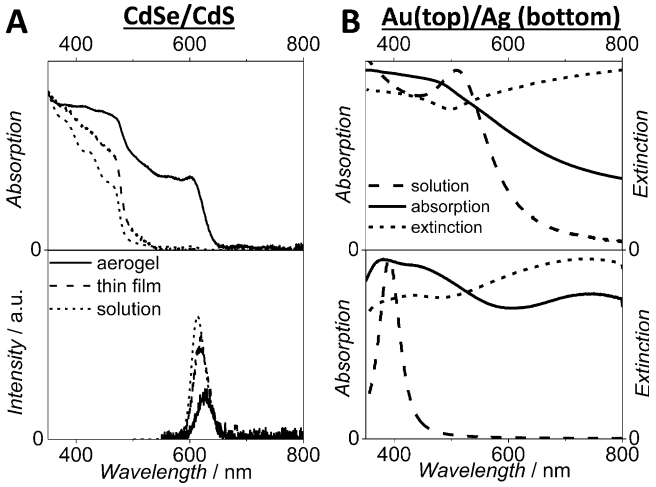

Figure 4. A) Spectroscopic investigation of the CdSe/CdS aerogels (top: absorption, bottom: emission spectra) determined by means of an integrating sphere. B) absorption (solid line) and extinction (long dashed line) spectra of the aerogels from Au (top) and Ag NPs (bottom).

nanorods (Figure 4A) exhibit fluorescence, and the band edges of CdSe and CdS are still recognizable in their absorption spectra. We observe a shift to longer wavelengths for both emission and absorption spectra, which we attribute to the interparticle interactions caused by the close proximity. A decrease in luminescence quantum yield in comparison to the aqueous NP solution is observed (from 24% to 14% for thin aerogel films and 4.8% for aerogel monoliths).

The absorption and extinction spectra of both Au and Ag aerogels (Figure 4B) show a drastic change in comparison to the pristine NP solutions (see the Supporting Information). However, most notably, the aerogels exhibit extinction and absorption maxima, which we attribute to localized surface plasmon resonances and interplasmon coupling.[31]

In conclusion, in the recent work we have shown the fabrication of aerogels of pure noble metal, metal oxide, and semiconductor NPs by freezing and subsequent freeze-drying. These aerogels are self-supporting, non-ordered, and highly voluminous structures, with a particle density similar to the respective colloidal solution, without any chemical gelation agent or difficult solvent exchange and removal step. If fabricated on substrates, oriented thin films can be achieved, and the cryogelation method also allows different desirable shaping of the monoliths. The resulting aerogels exhibit high specific surface areas with accessible NCs. The assembly method can partially retain the nanoscopic properties of suitable building blocks such as size quantization (including photoluminescence) and plasmonic behavior. The developed procedure is easy, fast and extremely versatile towards different materials, NP shapes, and surface ligands, and is likely expandable to many more aqueous colloidal NP systems.

Acknowledgements

N.C.B., A.F., S.S.-P., S.N., and J.P. are grateful for financial support from the German Federal Ministry of Education and Research (BMBF) within the framework of NanoMatFutur, support code 03X5525. I.K. and D.W.B. gratefully acknowledge financial support from the Deutsche Forschungsgemeinschaft (DFG, SPP1613). We also would like to thank Dr. Dirk Dorfs and Dominik Hinrichs for scientific discussions.

Keywords: aerogels · cryogels · noble metal nanoparticles · voluminous superstructures

How to cite: *Angew. Chem. Int. Ed.* **2016**, *55*, 1200–1203
Angew. Chem. **2016**, *128*, 1217–1221

[1] J. L. Mohanan, I. U. Arachchige, S. L. Brock, *Science* **2005**, *307*, 397–400.
[2] N. Hüsing, U. Schubert, *Angew. Chem. Int. Ed.* **1998**, *37*, 22–45; *Angew. Chem.* **1998**, *110*, 22–47.
[3] T. Hendel, V. Lesnyak, L. Kühn, A.-K. Herrmann, N. C. Bigall, L. Borchardt, S. Kaskel, N. Gaponik, A. Eychmüller, *Adv. Funct. Mater.* **2013**, *23*, 1903–1911.
[4] S. Sánchez-Paradinas, D. Dorfs, S. Friebe, A. Freytag, A. Wolf, N. C. Bigall, *Adv. Mater.* **2015**, *27*, 6152–6156.
[5] B. C. Tappan, S. A. Steiner III, E. P. Luther, *Angew. Chem. Int. Ed.* **2010**, *49*, 4544–4565; *Angew. Chem.* **2010**, *122*, 4648–4669.
[6] K. S. Krishna, C. S. S. Sandeep, R. Philip, M. Eswaramoorthy, *ACS Nano* **2010**, *4*, 2681–2688.
[7] S. Brock, H. Yu in *Aerogels Handbook* (Eds.: M. A. Aegerter, N. Leventis, M. M. Koebel), Springer, New York, **2011**, pp. 367–384.
[8] N. Leventis, *Acc. Chem. Res.* **2007**, *40*, 874–884.
[9] W. Liu, A.-K. Herrmann, N. C. Bigall, P. Rodriguez, D. Wen, M. Oezaslan, T. J. Schmidt, N. Gaponik, A. Eychmüller, *Acc. Chem. Res.* **2015**, *48*, 154–162.
[10] H. D. Gesser, P. C. Goswami, *Chem. Rev.* **1989**, *89*, 765–788.
[11] S. L. Brock, *Angew. Chem. Int. Ed.* **2009**, *48*, 7484–7486; *Angew. Chem.* **2009**, *121*, 7620–7622.
[12] S. S. Kistler, *Nature* **1931**, *127*, 741.
[13] S. L. Brock, I. U. Arachchige, K. K. Kalebaila, *Comments Inorg. Chem.* **2006**, *27*, 103–126.
[14] J. L. Mohanan, S. L. Brock, *J. Sol-Gel Sci. Technol.* **2006**, *40*, 341–350.
[15] H. Yu, R. Bellair, R. M. Kannan, S. L. Brock, *J. Am. Chem. Soc.* **2008**, *130*, 5054–5055.
[16] H. Yu, S. L. Brock, *ACS Nano* **2008**, *2*, 1563–1570.
[17] Q. Yao, S. L. Brock, *Inorg. Chem.* **2011**, *50*, 9985–9992.
[18] A.-K. Herrmann, P. Formanek, L. Borchardt, M. Klose, L. Giebeler, J. Eckert, S. Kaskel, N. Gaponik, A. Eychmüller, *Chem. Mater.* **2014**, *26*, 1074–1083.
[19] D. V. Talapin, R. Koeppe, S. Götzinger, A. Kornowski, J. M. Lupton, A. L. Rogach, O. Benson, J. Feldmann, H. Weller, *Nano Lett.* **2003**, *3*, 1677–1681.
[20] L. Carbone, C. Nobile, M. De Giorgi, F. D. Sala, G. Morello, P. Pompa, M. Hytch, E. Snoeck, A. Fiore, I. R. Franchini, M. Nadasan, A. F. Silvestre, L. Chiodo, S. Kudera, R. Cingolani, R. Krahne, L. Manna, *Nano Lett.* **2007**, *7*, 2942–2950.
[21] N. Leventis, C. Chidambareswarapattar, A. Bang, C. Sotiriou-Leventis, *ACS Appl. Mater. Interfaces* **2014**, *6*, 6872–6882.
[22] A. Eychmüller, *Angew. Chem. Int. Ed.* **2005**, *44*, 4839–4841; *Angew. Chem.* **2005**, *117*, 4917–4919.
[23] A. Kern, W. Eysel, Mineralogisch-Petrograph. Inst., Univ. Heidelberg, Germany **1993**.
[24] H. Zhang, I. Hussain, M. Brust, M. F. Butler, S. P. Rannard, A. I. Cooper, *Nat. Mater.* **2005**, *4*, 787–793.
[25] L. Qian, H. Zhang, *J. Chem. Technol. Biotechnol.* **2011**, *86*, 172–184.
[26] H. Moor, *Z. Zellforsch. Mikrosk. Anat.* **1964**, *62*, 546–580.
[27] D. Walsh, L. Arcelli, T. Ikoma, J. Tanaka, S. Mann, *Nat. Mater.* **2003**, *2*, 386–390.
[28] W. Liu, A.-K. Herrmann, D. Geiger, L. Borchardt, F. Simon, S. Kaskel, N. Gaponik, A. Eychmüller, *Angew. Chem. Int. Ed.* **2012**, *51*, 5743–5747; *Angew. Chem.* **2012**, *124*, 5841–5846.
[29] N. C. Bigall, A.-K. Herrmann, M. Vogel, M. Rose, P. Simon, W. Carrillo-Cabrera, D. Dorfs, S. Kaskel, N. Gaponik, A. Eychmüller, *Angew. Chem. Int. Ed.* **2009**, *48*, 9731–9734; *Angew. Chem.* **2009**, *121*, 9911–9915.
[30] A.-K. Herrmann, P. Formanek, L. Borchardt, M. Klose, L. Giebeler, J. Eckert, S. Kaskel, N. Gaponik, A. Eychmüller, *Chem. Mater.* **2014**, *26*, 1074–1083.
[31] W. R. Holland, D. G. Hall, *Phys. Rev. B* **1983**, *27*, 7765–7768.

Received: September 24, 2015
Revised: October 26, 2015
Published online: December 7, 2015

